
Accelerated Evaluation of Ollivier-Ricci Curvature Lower Bounds: Bridging Theory and Computation

Wonwoo Kang*

Department of Mathematics
University of Illinois, Urbana-Champaign
wonwook2@illinois.edu

Heehyun Park*

Department of Computer Science and Engineering
Pennsylvania State University
hbp5148@psu.edu

Abstract

Curvature serves as a potent and descriptive invariant, with its efficacy validated both theoretically and practically within graph theory. We employ a definition of generalized Ricci curvature proposed by Ollivier, which Lin and Yau later adapted to graph theory, known as Ollivier-Ricci curvature (ORC). ORC measures curvature using the Wasserstein distance, thereby integrating geometric concepts with probability theory and optimal transport. Jost and Liu previously discussed the lower bound of ORC by showing the upper bound of the Wasserstein distance. We extend the applicability of these bounds to discrete spaces with metrics on integers, specifically hypergraphs. Compared to prior work on ORC in hypergraphs by Coupette, Dalleiger, and Rieck, which faced computational challenges, our method introduces a simplified approach with linear computational complexity, making it particularly suitable for analyzing large-scale networks. Through extensive simulations and application to synthetic and real-world datasets, we demonstrate the significant improvements our method offers in evaluating ORC.

1 Introduction

Curvature serves as a fundamental and illuminating invariant, extensively validated both theoretically and empirically within the realm of graphs. In particular, the Ollivier-Ricci curvature (ORC) [16; 17] stands out as a key measure, offering insights into disparities observed in random walks through the perspective of Wasserstein distance. This geometric concept is deeply connected with principles from probability theory and optimal transport, enhancing our comprehension of complex network structures. It has also shown its usefulness in assessing disparities between real-world networks [19] and in finding bottlenecks in real-world networks [9].

The concept of the lower bound of ORC is crucial for practical computations, as it provides a simplified yet effective way to estimate curvature without the need for exhaustive calculations. This bound allows for a more efficient analysis of network structures, particularly in large-scale applications where computational resources are limited.

While the lower bounds of ORC have been explored in previous works by Jost and Liu [10], our research takes this foundational result further by generalizing it to broader contexts, including spaces with metrics on integers with elements of laziness incorporated into their structure. This extension broadens our theoretical framework, enabling it to accommodate a wider variety of computational scenarios and represents our primary theoretical contribution.

In practical terms, a significant application of our theoretical development is in the analysis of hypergraphs. Hypergraphs, which allow any number of nodes to participate in an edge, provide a more accurate representation of complex relationships. Examples of such relationships include

*Equal contributions, alphabetical order.

co-authorships in scientific publications [14; 24], intricate interactions among chemicals [4], and group dynamics in social conversations [11]. These scenarios, typically constrained by traditional graph models, can now be effectively modeled and analyzed through our extended approach to curvatures in hypergraphs.

Recent efforts have begun to explore the application of curvature to hypergraphs, recognizing their potential to capture multi-dimensional interactions [1; 5; 7; 12]. However, computing curvature in such settings is time-consuming, especially due to the numerical methods required to calculate Wasserstein distance. These methods often face scalability and computational efficiency issues when dealing with large and complex datasets, presenting significant barriers to their broad application in hypergraph analysis.

In response to the computational challenges presented by current curvature-driven techniques, our paper proposes a simplified approach with the extension of the upper bound of Wasserstein distance, which implies the lower bound of ORC, to hypergraphs. Extending the lower bound of ORC to hypergraphs presents an exciting opportunity to deepen our understanding of curvature in complex network structures with linear computational complexity. This method addresses the need for efficient algorithms capable of analyzing large-scale networks where traditional methods may be computationally prohibitive. By leveraging insights from ORC and adapting them to hypergraphs, our approach offers a practical solution for curvature analysis in real-world network applications.

Overall, our paper aims to contribute to the ongoing discourse on Ollivier-Ricci curvature by extending the lower bound of ORC to broader settings and presenting a computationally efficient approach. Through theoretical analysis and empirical validation, we demonstrate the effectiveness and applicability of our method in understanding complex network structures.

2 Backgrounds

2.1 Graph Theory

A graph $G = (V, E)$ consists of a set of vertices V and a set of edges E . Each edge $e \in E$ represents a pair of vertices, signifying a connection between them. In this literature, we concentrate on undirected graphs, where edges are unordered pairs. Two vertices u and v in V are adjacent (denoted $u \sim v$) if there is an edge $e = \{u, v\}$ connecting them directly. An edge e is also said to be adjacent to a vertex v if it connects v with another vertex u . Each vertex v in V is connected to a finite number of edges, characterizing the graph as locally finite. A simple graph permits no more than one edge between any pair of vertices, and does not allow any edge to connect a vertex to itself. A multigraph may include multiple edges connecting the same pair of vertices.

A simple hypergraph $H = (V, E)$ extends simple graphs, where each hyperedge $e \in E$ can connect any subset of vertices, up to $|V|$. A multihypergraph allows identical hyperedges to occur multiple times. The degree d_v of a vertex v is the number of edges connected to it, expressed as $d_v = |\{e \in E \mid v \in e\}|$. The neighborhood $\mathcal{N}(v)$ comprises all vertices adjacent to v . In simple graphs, $d_v = |\mathcal{N}(v)|$, whereas in multigraphs, $d_v \geq |\mathcal{N}(v)|$. Two vertices u and v are connected if there exists a sequence of adjacent vertices from u to v , known as a path. The distance $d(u, v)$ counts the number of edges in the path with the shortest cardinality.

In a weighted graph, each edge is assigned a numerical value or weight. The weight between two adjacent vertices u and v is denoted by w_{uv} , equal to w_{vu} in undirected graphs. For unweighted scenarios, this is typically set to $w_{uv} = 1$. The weighted degree of a vertex v is defined as $d_v = \sum_{u \sim v} w_{vu}$, representing the sum of the weights of the edges connected to v .

2.2 Metric Spaces on Integers

In this section, we only discuss a discrete space X . Metric spaces on integers are metric spaces (X, d) where the distance between any two points is an integer. These spaces are essential in discrete mathematics and theoretical computer science.

A key example is the graph distance in graphs, where distances between vertices, measured as the shortest path via edges, are integers. This property is central to graph theory and its applications. Another example is the l^1 norm on the integer lattice \mathbb{Z}^n , where the distance between any two points

is the sum of the absolute differences of their coordinates:

$$d(x, y) = \sum_{i=1}^n |x_i - y_i|,$$

ensuring integer distances. Additionally, the Hamming distance in coding theory measures the number of differing positions between two equal-length binary strings, providing a metric on integers critical for error detection and correction.

2.3 Ollivier’s Ricci Curvature

Ricci curvature serves as a foundational concept within Riemannian geometry, describing how a curve or a surface diverges from being straight or flat [18]. Within this mathematical framework, curvatures like Ricci curvature offer valuable insights into the distinct geometric properties of various spaces. Naturally, there arose an inclination to seek analogous principles applicable to metric spaces beyond Riemannian manifolds [10].

In the context of graph theory, such generalized curvatures are relatively straightforward to define and assess [13; 21]. Moreover, they illuminate various quantities introduced in network analysis, offering a clearer conceptual foundation compared to other measures [15; 20]. Among these generalized curvatures, Forman [8] introduced the Ricci curvature for simplicial complexes, which stands out as the simplest.

Ollivier [16] also extended the concept of Ricci curvature from smooth manifold theory to the realm of general metric spaces. This work has established another way to analyze the curvature properties in spaces that are different from Riemannian manifolds. At the heart of Ollivier’s Ricci curvature (ORC) lies the idea of contrasting the cost of transporting probability measures within a metric space. This concept borrows heavily from optimal transport theory.

The Wasserstein distance is a fundamental metric in the field of optimal transport theory, providing a measure of the dissimilarity between two probability distributions [3; 22; 23]. This distance quantifies the minimal *work* needed to transform one distribution into another. Specifically, for probability measures μ and ν on a metric space (X, d) , the Wasserstein distance $W_1(\mu, \nu)$ is formally defined as follows:

$$W_1(\mu, \nu) = \inf_{\gamma \in \Gamma(\mu, \nu)} \int_{X \times X} d(x, y) d\gamma(x, y). \quad (1)$$

Here, $\Gamma(\mu, \nu)$ represents the set of all joint probability measures on $X \times X$ that have marginals μ and ν , respectively. Thus, for all subsets A, B of X , the measure γ satisfies $\gamma(A \times X) = \mu(A)$ and $\gamma(X \times B) = \nu(B)$. The measure γ essentially encodes an *optimal transport plan*, detailing how mass is transferred from one distribution to the other.

In standard Riemannian geometry, Ricci curvature provides insight into how the volume of infinitesimal geodesic balls changes when transported along parallel paths. Ollivier’s approach shifts the focus from volume displacement to the dynamics of probability distributions, quantifying curvature by measuring the evolution of distances between distributions as they are transported along a geodesic. This provides a comprehensive understanding of geometric structures in spaces where traditional methods may not apply.

Definition 1 (Ollivier’s Ricci curvature). *In a general metric space (X, d) equipped with a local probability measure $\mu_x(\cdot)$ at each point $x \in X$, the structure is denoted by (X, d, μ) . The Ollivier Ricci curvature $\kappa(x, y)$ between any two points $x, y \in X$ is defined by the formula:*

$$\kappa(x, y) = 1 - \frac{W_1(\mu_x, \mu_y)}{d(x, y)} \quad (2)$$

Here, μ_x and μ_y are the local probability measures at points x and y , respectively, which represent the distribution of mass around these points within the space.

Also, for an edge $e = (x, y)$, we will use $\kappa(e)$ as a shorthand notation. In graph theory, the application of the Wasserstein distance aids in comprehending the overall structure of a graph via its local curvature properties. In the graph setting, a probability measure μ_x is assigned to each vertex

$x \in V$, defined as follows:

$$\mu_x(y) = \begin{cases} \frac{w_{xy}}{d_x} & \text{if node } y \text{ is connected to node } x \\ 0 & \text{otherwise} \end{cases} \quad (3)$$

Here, the weighted degree d_x is $d_x = \sum_{y \sim x} w_{xy}$, summing the weights of all edges connected to vertex x . In the case of unweighted graphs, the weighted degree d_x becomes simply the number of edges connected to vertex x , which is the traditional degree of the vertex. Accordingly, the probability measure μ_x for an unweighted graph is defined as:

$$\mu_x(y) = \begin{cases} \frac{1}{d_x} & \text{if node } y \text{ is connected to node } x \\ 0 & \text{otherwise} \end{cases} \quad (4)$$

This adjustment reflects that each adjacent vertex has an equal probability of being chosen, simplifying the understanding and computation of probability distributions in the context of unweighted graphs. Consequently, the Wasserstein distance between the measures at vertices x and y is defined by

$$W_1(\mu_x, \mu_y) = \inf_{\gamma} \sum_{x' \sim x} \sum_{y' \sim y} d(x', y') \gamma(x', y') \quad (5)$$

where γ represents a transport plan between the distributions μ_x and μ_y , minimizing the total distance required to transport mass from the neighborhood of x to that of y . The sums run over all vertices x' adjacent to x and y' adjacent to y , and $d(x', y')$ denotes the distance between vertices x' and y' .

We can delve deeper into the analytical methods used to quantify the transportation of these measures across the graph. An essential tool for this analysis is *Kantorovich duality*, which provides a powerful framework for deducing bounds on the Wasserstein distance, linking local interactions to global geometric properties of the graph [22].

Proposition 1 (Kantorovich Duality).

$$W_1(\mu_x, \mu_y) = \sup_{f, 1\text{-Lip}} \left[\sum_{z, z \sim x} f(z) \mu_x(z) - \sum_{z, z \sim y} f(z) \mu_y(z) \right]$$

where the supremum is taken over all 1-Lipschitz continuous functions on $G = (V, E)$, i.e., functions $f : V \rightarrow \mathbb{R}$ such that

$$|f(x) - f(y)| \leq d(x, y)$$

for any $x, y \in V$, $x \neq y$.

With Proposition 1, by strategically selecting a suitable 1-Lipschitz function f , we can effectively find a lower bound for W_1 and, consequently, an upper bound for the curvature measure κ . This duality and its implications highlight the interconnectedness of local vertex measures and the broader structural characteristics they influence.

3 Lower Bound of ORC

Accurate measurement of curvature demands significant computational cost. The Sinkhorn algorithm, which computes the Wasserstein distance, is time-intensive due to its dependence on the number of iterations and convergence radius. For applications such as machine learning and clustering, a rapid estimation of curvature using simple graph statistics, such as degrees, would be more efficient.

Not only in graphs, but also in the discrete space with metrics on integers mentioned in Section 2.2, curvature can be discussed. Let us assume that space X is a discrete space and the metric d is defined only on integers.

3.1 Lower Bound of ORC on Spaces with Metrics on Integers

In a space (X, d) with metrics $d(\cdot, \cdot)$ on integers equipped with local probability measures $\mu_x(\cdot)$ for each point $x \in X$, these measures can be conceptualized as a distribution of transition probabilities in a random walk. Here, μ_x represents the probability of transitioning from point x to other points within the space X .

Based on the results presented in [10], we can further generalize this approach. They defined the local measure μ_x for a given graph as expressed in (3), but this can be extended to spaces with metrics on integers, such as integer lattices with ℓ^1 norm and strings of equal length with the Hamming distance. Complete proofs of this extension and results related to graphs can be found in Appendix A.

Define $(x)_+$ as x if $x \geq 0$ and 0 otherwise. An important observation is that the curvature $\kappa(x, y)$ exhibits symmetry in terms of x and y . To facilitate our discussion, we introduce two operations:

$$a \wedge b = \min\{a, b\}, \quad a \vee b = \max\{a, b\}.$$

Theorem 1. *In a metric space (X, d) with metrics $d(\cdot, \cdot)$ on \mathbb{Z} equipped with local probability measures $\mu_x(\cdot)$ for each point $x \in X$, for any adjacent pair of elements $x, y \in X$,*

$$\begin{aligned} W_1(\mu_x, \mu_y) \leq & 1 + \left(\left(1 - \mu_x(y) - \mu_y(x) - \sum_{z, z \sim x, z \sim y} \mu_x(z) \vee \mu_y(z) \right)_+ \right. \\ & \left. + \left(1 - \mu_x(y) - \mu_y(x) - \sum_{z, z \sim x, z \sim y} \mu_x(z) \wedge \mu_y(z) \right)_+ - \sum_{z, z \sim x, z \sim y} \mu_x(z) \wedge \mu_y(z) \right). \end{aligned}$$

Hence, we get

$$\begin{aligned} \kappa(x, y) \geq & \left(- \left(1 - \mu_x(y) - \mu_y(x) - \sum_{z, z \sim x, z \sim y} \mu_x(z) \vee \mu_y(z) \right)_+ \right. \\ & \left. - \left(1 - \mu_x(y) - \mu_y(x) - \sum_{z, z \sim x, z \sim y} \mu_x(z) \wedge \mu_y(z) \right)_+ + \sum_{z, z \sim x, z \sim y} \mu_x(z) \wedge \mu_y(z) \right). \end{aligned}$$

3.2 Curvature with Laziness

A lazy random walk is closely related to how it resists movement from its current state. A point x in this space can be considered lazy if its associated measure μ_x is heavily concentrated around x itself, indicating a high probability of remaining at the same point in successive transitions. This method combines ideas from the geometry of spaces and random processes. In the context of optimal transport, the laziness of a point is reflected by the Wasserstein distance, where a high distance to other measures indicates a reluctance to move away from the current state.

To quantify the laziness as discussed in the context of a metric space (X, d) with local probability measures μ_x , we can introduce a parameter $\alpha \in (0, 1)$. This parameter α will serve as a numerical representation of the degree of laziness at each point in the space. We then describe a lazy local measure μ_x^α of μ_x as

$$\mu_x^\alpha = \alpha \delta_x + (1 - \alpha) \mu_x$$

where δ_x is the Dirac measure concentrated at x . We can extend the results of Wasserstein and ORC in α -lazy random walks on graphs from [13] to discrete spaces (X, d) with metrics on integers.

Theorem 2. *Let (X, d) be a space with metrics on \mathbb{Z} with a local probability measure $\mu_x(\cdot)$ for each $x \in X$. For any adjacent $x, y \in X$, let μ_x^α and μ_y^α be the lazy versions of μ_x and μ_y for the lazy parameter $\alpha \in (0, 1)$, respectively. Then,*

$$W_1(\mu_x^\alpha, \mu_y^\alpha) \leq (1 - \alpha)W_1(\mu_x, \mu_y) + \alpha.$$

Corollary 1. *Let (X, d) be a space with metrics on \mathbb{Z} with a local probability measure $\mu_x(\cdot)$ for each $x \in X$. For any adjacent $x, y \in X$, let μ_x^α and μ_y^α be the lazy versions of μ_x and μ_y for the lazy parameter $\alpha \in (0, 1)$, respectively. Let $\kappa(x, y)$ be the Ricci curvature on (X, d, μ) and $\kappa^\alpha(x, y)$ be the Ricci curvature on (X, d, μ^α) between x and y , then*

$$\kappa^\alpha(x, y) \geq (1 - \alpha)\kappa(x, y). \quad (6)$$

3.3 Lower bounds of ORC

From the results of the two subsections above, we can ultimately generalize to local measures that incorporate elements of laziness in a space (X, d) . By combining the results of Theorem 1 and Theorem 2, we can summarize as follows.

Theorem 3. *In a metric space (X, d) with metric $d(\cdot, \cdot)$ on \mathbb{Z} equipped with local probability measures $\mu_x(\cdot)$ for each point $x \in X$, for any adjacent pair of elements $x, y \in X$, without loss of generality assume $\mu_x(x) \leq \mu_y(y)$. $\mu_x(x)$ can be considered as laziness, and let ν_x and ν_y be the measures obtained by excluding laziness from μ_x and μ_y and renormalizing them. Then,*

$$W_1(\mu_x, \mu_y) \leq \mu_x(x) + (1 - \mu_x(x)) \left(1 + \left(1 - \nu_x(y) - \nu_y(x) - \sum_{z, z \sim x, z \sim y} \nu_x(z) \vee \nu_y(z) \right)_+ \right. \\ \left. + \left(1 - \nu_x(y) - \nu_y(x) - \sum_{z, z \sim x, z \sim y} \nu_x(z) \wedge \nu_y(z) \right)_+ - \sum_{z, z \sim x, z \sim y} \nu_x(z) \wedge \nu_y(z) \right).$$

Hence, we get

$$\kappa(x, y) \geq (1 - \mu_x(x)) \left(- \left(1 - \nu_x(y) - \nu_y(x) - \sum_{z, z \sim x, z \sim y} \nu_x(z) \vee \nu_y(z) \right)_+ \right. \\ \left. - \left(1 - \nu_x(y) - \nu_y(x) - \sum_{z, z \sim x, z \sim y} \nu_x(z) \wedge \nu_y(z) \right)_+ + \sum_{z, z \sim x, z \sim y} \nu_x(z) \wedge \nu_y(z) \right).$$

4 Algorithm

From Theorem 3, we can develop an algorithm to evaluate the upper bound of the Wasserstein distance. Reviewing the formula once more, given two adjacent elements x and y , along with their local probability measures μ_x and μ_y , the goal is to find the upper bound of $W_1(\mu_x, \mu_y)$. From the inequality in the theorem, we can see that only a single iteration is needed. Therefore, the time complexity is $O(n)$, where n is the number of vertices. See Algorithm 1.

Algorithm 1 Estimate Wasserstein Distance

```

1: procedure WASSERSTEIN( $x, y, \mu_x, \mu_y$ )
2:    $\alpha \leftarrow \min(\mu_x(x), \mu_y(y))$ 
3:    $\nu_x \leftarrow \frac{1}{1-\alpha}(\mu_x - \alpha\delta_x)$ 
4:    $\nu_y \leftarrow \frac{1}{1-\alpha}(\mu_y - \alpha\delta_y)$ 
5:    $\text{maxSum} \leftarrow 0$ 
6:    $\text{minSum} \leftarrow 0$ 
7:   for all  $v \in V$  do
8:      $\text{maxSum} \leftarrow \text{maxSum} + \max(\nu_x(v), \nu_y(v))$ 
9:      $\text{minSum} \leftarrow \text{minSum} + \min(\nu_x(v), \nu_y(v))$ 
10:  end for
11:   $W \leftarrow 1 - \text{minSum}$ 
12:  if  $1 - \nu_x(y) - \nu_y(x) - \text{maxSum} > 0$  then
13:     $W \leftarrow W + (1 - \nu_x(y) - \nu_y(x) - \text{maxSum})$ 
14:  end if
15:  if  $1 - \nu_x(y) - \nu_y(x) - \text{minSum} > 0$  then
16:     $W \leftarrow W + (1 - \nu_x(y) - \nu_y(x) - \text{minSum})$ 
17:  end if
18:   $W \leftarrow \alpha + (1 - \alpha)W$ 
19:  return  $W$ 
20: end procedure

```

5 Application: Curvature in Hypergraphs

In the previous section, we noted that we can establish a minimum estimate for ORC from a maximum estimate for the Wasserstein distance for any spaces with metrics on integers equipped with local

probability measures. We will now apply Wasserstein distance estimation for specific measures to hypergraphs and assess their suitability for various scenarios.

In hypergraphs, an edge can have multiple cardinalities, so it should not be considered merely as a pair of nodes as in traditional graphs. Therefore, the method of calculating the lower bound of ORC as discussed by Jost and Liu [10] cannot be intuitively applied. Recently, a new framework for defining curvature in hypergraphs was discussed by Coupette, Dalleiger, and Rieck [5].

In the given hypergraphs, we shall first define the local measures. Their work introduced three methods for defining measures with mathematical implications. Since our Wasserstein distance estimation is generalized for well-defined local measures, it can be applied to all these methods and potentially to other measures based on different mathematical intuitions.

They also defined a new function called the Aggregation (AGG) function for each edge, taking into account the concept of optimal transport where Wasserstein aggregates probabilities. The aggregate function is a function that replaces the traditional Wasserstein distance for edges in hypergraphs with a cardinality of 2 or more. There are three types of AGG functions defined in [5], AGG_A , AGG_B , and AGG_M . The subscripts A, B, and M stand for average, barycenter, and maximum, respectively.

Now, based on the given or our defined AGG function, we can define the curvature for a specific edge as follows.

$$\kappa(e) = 1 - AGG(e)$$

This is similar to the method used in graphs, where ORC was determined through the Wasserstein distance. In Appendix B, we will discuss local measures, AGG functions, and different curvatures with our new Wasserstein distance in greater detail.

The aggregate function and curvature ultimately require evaluating the Wasserstein distance. Here, instead of using traditional methods to compute the Wasserstein distance, we apply our approach. For details about the experiments, please refer to Section 6.

6 Experiments

The experiments were conducted in two main parts. First, we compared the time required for our algorithm versus the numerical method called the Sinkhorn algorithm across various datasets. The second part involved comparing the curvatures obtained from the two algorithms for each dataset. For details on the datasets and the experimental setup, please refer to Appendix C.

6.1 Time Evaluation

We performed a visual examination of the computational time required to compute the Wasserstein distance across multiple datasets (see Figure 1). The time data, measured in milliseconds, was plotted on a **logarithmic scale**. Experiments were conducted under two settings, with blue bars representing the time taken by the traditional method and orange bars representing the time taken by our method.

Our analysis revealed a noteworthy decrease in computational time compared to conventional algorithms. Typically, traditional methods iterate numerically until the results converge within a specified radius or until reaching a predetermined number of iterations. In contrast, our algorithm completes the computation in a single iteration, leading to significant time savings, as confirmed by our experimental findings. This efficiency gain is crucial, particularly in applications involving large-scale datasets where computational resources and time are critical factors.

6.2 Curvature Evaluation

In Figure 2, we present curvatures generated by both traditional and our algorithms across different datasets on scatter graphs. The x-axis shows curvatures from our algorithm, while the y-axis shows those from the traditional method. The red line represents the trend line, and the black dotted line indicates the ideal $y = x$ line, serving as a benchmark for comparison.

The accompanying histogram to the right provides further insight into the distribution of curvature values. Red bars represent outcomes from traditional methods, while blue bars denote our results. Despite a downward shift in the red bars compared to the blue bars, the overall shape of the distribution remains consistent.

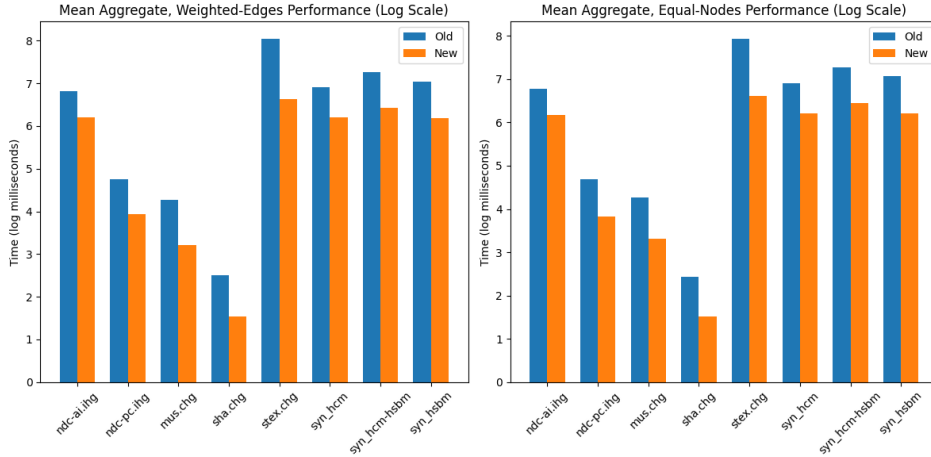


Figure 1: Logarithmic scale graph showing the time evaluation for computing the Wasserstein distance across different datasets.

Our approach calculates the lower bound of curvatures, resulting in a general downward shift compared to conventional methods. However, this shift does not significantly affect the overall distribution shape. In machine learning applications, such as community detection or clustering, determining a threshold curvature to define a community is crucial. The observed shift does not pose a significant issue, as the relative differences and distribution shapes are maintained.

These visual representations allow us to assess the impact of our methodology compared to conventional approaches. The data demonstrates that while our method produces lower values, it preserves the integrity of the data distribution.

This observation is significant, as it confirms that while our curvatures are systematically lower, they remain functionally comparable for tasks requiring the identification of structural characteristics within data, such as detecting tightly-knit communities or clusters.

7 Limitations and Conclusions

While our study presents promising results, it is crucial to acknowledge certain limitations that surfaced during our analysis. Particularly, we observed instances where the translation of data was not uniform across all datasets, leading to significant discrepancies in certain cases. Despite these variations, our novel methodology continued to demonstrate effectiveness, particularly in discerning the threshold of curvature—a critical aspect in the realm of community detection. By maintaining its efficacy in this fundamental aspect, our approach reaffirms its relevance and applicability in addressing key challenges within network analysis.

Looking ahead, our future research endeavors will focus on further refining and expanding the scope of our theory. First, in the proof of the main theorem, we only considered the scenario where the curvature decreases with points shared by two vertices. This corresponds to the geometric implication that the curvature decreases in a triangular configuration in a discrete graph. However, as discussed by Topping et al. [21], refining our estimation to include cases involving grids, squares, or pentagons would yield even better results. Furthermore, we discussed the theoretical implications of considering laziness in our work. Still, we aim to evaluate its performance under different scenarios, such as employing α -lazy random walks, to gain deeper insights into its robustness and adaptability. Additionally, we intend to extend our theoretical framework to encompass directed graphs or spaces with metrics on real numbers, thus broadening the applicability of our methodology and paving the way for more comprehensive analyses in diverse network structures. Through these endeavors, we aim to not only address existing limitations but also advance the theoretical foundations of curvature evaluation, contributing to the ongoing development of network science.

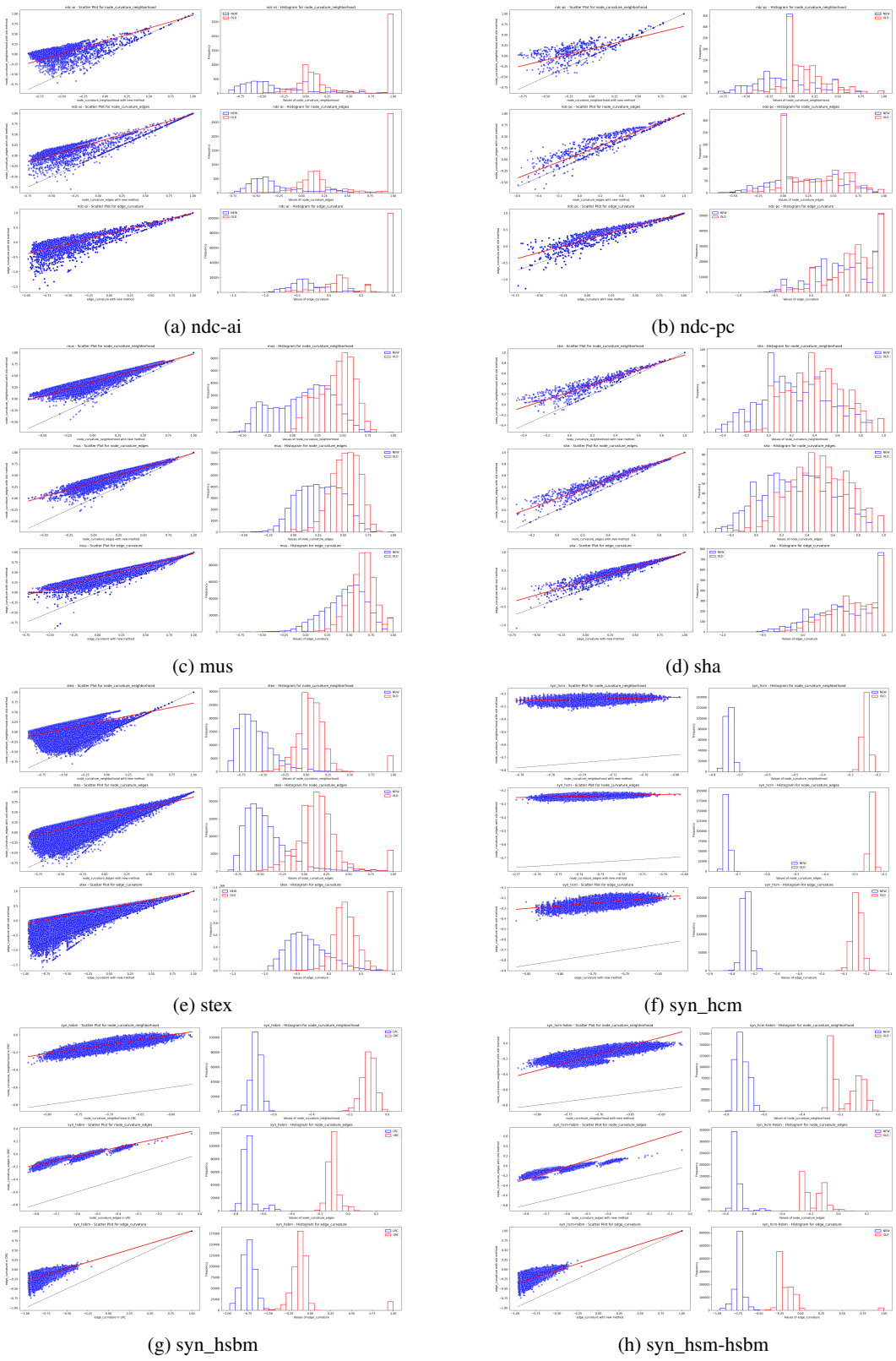


Figure 2: Evaluations of curvatures

Acknowledgements

The authors wish to express their sincere gratitude to Chonghan Lee at Pennsylvania State University for his valuable advice and insights regarding the experimental procedures discussed in this paper.

References

- [1] S. Asoodeh, T. Gao, and J. Evans. Curvature of hypergraphs via multi-marginal optimal transport. pages 1180–1185, 2018. doi: 10.1109/CDC.2018.8619706.
- [2] A. Banerjee. On the spectrum of hypergraphs. *Linear Algebra and its Applications*, 614:82–110, 2021. ISSN 0024-3795. doi: <https://doi.org/10.1016/j.laa.2020.01.012>. Special Issue ILAS 2019.
- [3] R. Bott, A. Jaffe, D. Jerison, G. Lusztig, I. Singer, and S. T. Yau, editors. *Current developments in mathematics, 1997*. International Press, Boston, MA, 1999. ISBN 1-57146-078-0. Papers from the conference held in Cambridge, MA, 1997.
- [4] G. Burgio, J. T. Matamalas, S. Gómez, and A. Arenas. Evolution of cooperation in the presence of higher-order interactions: From networks to hypergraphs. *Entropy*, 22(7), 2020. ISSN 1099-4300. doi: 10.3390/e22070744.
- [5] C. Coupette, S. Dalleiger, and B. Rieck. Ollivier-ricci curvature for hypergraphs: A unified framework. In *The Eleventh International Conference on Learning Representations, ICLR 2023, Kigali, Rwanda, May 1-5, 2023*. OpenReview.net, 2023.
- [6] C. Coupette, J. Vreeken, and B. Rieck. All the world’s a (hyper) graph: A data drama. *Digital Scholarship in the Humanities*, 39(1):74–96, 2024.
- [7] M. Eidi and J. Jost. Ollivier ricci curvature of directed hypergraphs. *Scientific Reports*, 10(1): 12466, 2020.
- [8] R. Forman. Bochner’s method for cell complexes and combinatorial Ricci curvature. *Discrete & Computational Geometry. An International Journal of Mathematics and Computer Science*, 29(3):323–374, 2003. ISSN 0179-5376.
- [9] A. Gosztolai and A. Arnaudon. Unfolding the multiscale structure of networks with dynamical ollivier-ricci curvature. *Nature Communications*, 12(1):4561, 2021. doi: 10.1038/s41467-021-24884-1.
- [10] J. Jost and S. Liu. Ollivier’s Ricci curvature, local clustering and curvature-dimension inequalities on graphs. *Discrete & Computational Geometry. An International Journal of Mathematics and Computer Science*, 51(2):300–322, 2014. ISSN 0179-5376.
- [11] S. Kim, S. Kang, F. Bu, S. Y. Lee, J. Yoo, and K. Shin. Hypeboy: Generative self-supervised representation learning on hypergraphs. In *The Twelfth International Conference on Learning Representations*. OpenReview.net, 2024.
- [12] W. Leal, M. Eidi, and J. Jost. Ricci curvature of random and empirical directed hypernetworks. *Applied Network Science*, 5(1):65, 2020. doi: 10.1007/s41109-020-00309-8. URL <https://doi.org/10.1007/s41109-020-00309-8>.
- [13] Y. Lin, L. Lu, and S.-T. Yau. Ricci curvature of graphs. *The Tohoku Mathematical Journal. Second Series*, 63(4):605–627, 2011. ISSN 0040-8735.
- [14] R. Lung, N. Gaskó, and M. Suciú. A hypergraph model for representing scientific output. *Scientometrics*, 117, 09 2018. doi: 10.1007/s11192-018-2908-2.
- [15] C.-C. Ni, Y.-Y. Lin, J. Gao, X. D. Gu, and E. Saucan. Ricci curvature of the internet topology. In *2015 IEEE conference on computer communications (INFOCOM)*, pages 2758–2766. IEEE, 2015.
- [16] Y. Ollivier. Ricci curvature of metric spaces. *Comptes Rendus Mathématique. Académie des Sciences. Paris*, 345(11):643–646, 2007. ISSN 1631-073X.

- [17] Y. Ollivier. Ricci curvature of Markov chains on metric spaces. *Journal of Functional Analysis*, 256(3):810–864, 2009. ISSN 0022-1236.
- [18] G. Ricci-Curbastro. Direzioni e invarianti principali in una varietà qualunque. *Atti del Reale Istituto veneto di scienze, lettere ed arti*, 63(2):1233–1239, 1903-1904.
- [19] A. Samal, R. P. Sreejith, J. Gu, S. Liu, E. Saucan, and J. Jost. Comparative analysis of two discretizations of ricci curvature for complex networks. *Scientific Reports*, 8(1):8650, 2018. doi: 10.1038/s41598-018-27001-3.
- [20] R. Sandhu, T. Georgiou, E. Reznik, L. Zhu, I. Kolesov, Y. Senbabaoglu, and A. Tannenbaum. Graph curvature for differentiating cancer networks. *Scientific reports*, 5(1):12323, 2015.
- [21] J. Topping, F. Di Giovanni, B. P. Chamberlain, X. Dong, and M. M. Bronstein. Understanding over-squashing and bottlenecks on graphs via curvature. *arXiv preprint arXiv:2111.14522*, 2021.
- [22] C. Villani. *Topics in optimal transportation*, volume 58 of *Graduate Studies in Mathematics*. American Mathematical Society, Providence, RI, 2003. ISBN 0-8218-3312-X. doi: 10.1090/gsm/058.
- [23] C. Villani. *Optimal transport*, volume 338 of *Grundlehren der mathematischen Wissenschaften [Fundamental Principles of Mathematical Sciences]*. Springer-Verlag, Berlin, 2009. ISBN 978-3-540-71049-3. doi: 10.1007/978-3-540-71050-9. Old and new.
- [24] W. Wang, T. Tang, F. Xia, Z. Gong, Z. Chen, and H. Liu. Collaborative filtering with network representation learning for citation recommendation. *IEEE Transactions on Big Data*, PP:1–1, 10 2020. doi: 10.1109/TBDATA.2020.3034976.

A Proofs

A.1 Proofs of Theorems in Section 3

Theorem 1. *In a metric space (X, d) with metrics $d(\cdot, \cdot)$ on \mathbb{Z} equipped with local probability measures $\mu_x(\cdot)$ for each point $x \in X$, for any adjacent pair of elements $x, y \in X$,*

$$W_1(\mu_x, \mu_y) \leq 1 + \left(\left(1 - \mu_x(y) - \mu_y(x) - \sum_{z, z \sim x, z \sim y} \mu_x(z) \vee \mu_y(z) \right)_+ \right. \\ \left. + \left(1 - \mu_x(y) - \mu_y(x) - \sum_{z, z \sim x, z \sim y} \mu_x(z) \wedge \mu_y(z) \right)_+ - \sum_{z, z \sim x, z \sim y} \mu_x(z) \wedge \mu_y(z) \right).$$

Hence, we get

$$\kappa(x, y) \geq \left(- \left(1 - \mu_x(y) - \mu_y(x) - \sum_{z, z \sim x, z \sim y} \mu_x(z) \vee \mu_y(z) \right)_+ \right. \\ \left. - \left(1 - \mu_x(y) - \mu_y(x) - \sum_{z, z \sim x, z \sim y} \mu_x(z) \wedge \mu_y(z) \right)_+ + \sum_{z, z \sim x, z \sim y} \mu_x(z) \wedge \mu_y(z) \right).$$

Remark. The proof follows the same logic as the proof of Theorem 3 in [10], so the reader might find this proof very similar, with differences in some settings. The point of this proof is to show how a similar proof works in our setting.

Proof. In principle, our transfer plan moving μ_x to μ_y should be as follows. First, we move the mass of $\mu_x(y)$ from y to own neighbors of y ; second, we move a mass of $\mu_y(x)$ from own neighbors of x to x ; finally, fill gaps using the mass at own neighbors of x or common neighbors. Filling the gaps at common neighbors costs 2 and the ones at own neighbors of y costs 3.

The first step can be realized, i.e. the total mass of own neighbors of y is at least a mass of $\mu_x(y)$, when

$$1 - \mu_y(x) - \sum_{z, z \sim x, z \sim y} \mu_x(z) \vee \mu_y(z) \geq \mu_x(y)$$

or

$$A := 1 - \mu_y(x) - \mu_x(y) - \sum_{z, z \sim x, z \sim y} \mu_x(z) \vee \mu_y(z) \geq 0.$$

The second step can be realized, i.e. the total mass of own neighbors of x is at least $\mu_y(x)$, when

$$1 - \mu_x(y) - \sum_{z, z \sim x, z \sim y} \mu_x(z) \wedge \mu_y(z) \geq \mu_y(x)$$

or

$$B := 1 - \mu_y(x) - \mu_x(y) - \sum_{z, z \sim x, z \sim y} \mu_x(z) \wedge \mu_y(z) \geq 0.$$

Obviously, $A \leq B$. If $0 \leq A \leq B$,

$$\begin{aligned} W_1(\mu_x, \mu_y) &\leq \mu_x(y) \times 1 + \mu_y(x) \times 1 + \sum_{z, z \sim x, z \sim y} (\mu_x(z) \vee \mu_y(z) - \mu_x(z) \wedge \mu_y(z)) \times 2 \\ &+ \left(1 - \mu_x(y) - \mu_y(x) - \sum_{z, z \sim x, z \sim y} (\mu_x(z) \vee \mu_y(z) - \mu_x(z) \wedge \mu_y(z)) \right. \\ &\quad \left. - \sum_{z, z \sim x, z \sim y} \mu_x(z) \wedge \mu_y(z) \right) \times 3 \\ &= 3 - 2\mu_x(y) - 2\mu_y(x) - \sum_{z, z \sim x, z \sim y} \mu_x(z) \vee \mu_y(z) - 2 \sum_{z, z \sim x, z \sim y} \mu_x(z) \wedge \mu_y(z) \\ &= 1 + \left(\left(1 - \mu_x(y) - \mu_y(x) - \sum_{z, z \sim x, z \sim y} \mu_x(z) \vee \mu_y(z) \right)_+ \right. \\ &\quad \left. + \left(1 - \mu_x(y) - \mu_y(x) - \sum_{z, z \sim x, z \sim y} \mu_x(z) \wedge \mu_y(z) \right)_+ - \sum_{z, z \sim x, z \sim y} \mu_x(z) \wedge \mu_y(z) \right) \end{aligned}$$

which is the desired result. Indeed, the terms inside $(\cdot)_+$ operations are valid since A and B are non-negative. In conclusion, using the fact from (2) that $\kappa(x, y) = 1 - W_1(\mu_x, \mu_y)$,

$$\kappa(x, y) \geq -2 + 2\mu_x(y) + 2\mu_y(x) + \sum_{z, z \sim x, z \sim y} \mu_x(z) \vee \mu_y(z) + 2 \sum_{z, z \sim x, z \sim y} \mu_x(z) \wedge \mu_y(z)$$

when $0 \leq A \leq B$.

If $A < 0 \leq B$, we do not need the part where it costs 3, because the mass $\mu_x(y)$ will fill all own neighbor of y . Hence,

$$\begin{aligned} W_1(\mu_x, \mu_y) &\leq \mu_x(y) \times 1 + \mu_y(x) \times 1 + \left(1 - \mu_x(y) - \mu_y(x) - \sum_{z, z \sim x, z \sim y} \mu_x(z) \wedge \mu_y(z) \right) \times 2 \\ &= 2 - \mu_x(y) - \mu_y(x) - \sum_{z, z \sim x, z \sim y} \mu_x(z) \wedge \mu_y(z) \times 2 \\ &= 1 + \left(\left(1 - \mu_x(y) - \mu_y(x) - \sum_{z, z \sim x, z \sim y} \mu_x(z) \vee \mu_y(z) \right)_+ \right. \\ &\quad \left. + \left(1 - \mu_x(y) - \mu_y(x) - \sum_{z, z \sim x, z \sim y} \mu_x(z) \wedge \mu_y(z) \right)_+ - \sum_{z, z \sim x, z \sim y} \mu_x(z) \wedge \mu_y(z) \right) \end{aligned}$$

In this case, $\left(1 - \mu_x(y) - \mu_y(x) - \sum_{z, z \sim x, z \sim y} \mu_x(z) \vee \mu_y(z)\right)_+$ is zero since A is negative, so the last equality still holds.

This implies that the curvature κ is,

$$\kappa(x, y) \geq -1 + \mu_x(y) + \mu_y(x) + 2 \sum_{z, z \sim x, z \sim y} \mu_x(z) \wedge \mu_y(z)$$

when $A < 0 \leq B$.

If $A \leq B < 0$, this implies we do not even need the part where it costs 2, because moving $\mu_x(y)$ in y and moving $\mu_y(x)$ from own neighbors of x will be sufficient. Therefore,

$$\begin{aligned} W_1(\mu_x, \mu_y) &\leq 1 - \sum_{z, z \sim x, z \sim y} \mu_x(z) \wedge \mu_y(z) \\ &= 1 + \left(\left(1 - \mu_x(y) - \mu_y(x) - \sum_{z, z \sim x, z \sim y} \mu_x(z) \vee \mu_y(z) \right)_+ \right. \\ &\quad \left. + \left(1 - \mu_x(y) - \mu_y(x) - \sum_{z, z \sim x, z \sim y} \mu_x(z) \wedge \mu_y(z) \right)_+ - \sum_{z, z \sim x, z \sim y} \mu_x(z) \wedge \mu_y(z) \right) \end{aligned}$$

since A and B are negative, which means both terms in $(\cdot)_+$ operation is zero.

So the curvature κ is

$$\kappa(x, y) \geq \sum_{z, z \sim x, z \sim y} \mu_x(z) \wedge \mu_y(z)$$

when $A \leq B < 0$.

For all cases, we have

$$\begin{aligned} W_1(\mu_x, \mu_y) &\leq 1 + \left(\left(1 - \mu_x(y) - \mu_y(x) - \sum_{z, z \sim x, z \sim y} \mu_x(z) \vee \mu_y(z) \right)_+ \right. \\ &\quad \left. + \left(1 - \mu_x(y) - \mu_y(x) - \sum_{z, z \sim x, z \sim y} \mu_x(z) \wedge \mu_y(z) \right)_+ - \sum_{z, z \sim x, z \sim y} \mu_x(z) \wedge \mu_y(z) \right) \end{aligned}$$

, and hence,

$$\begin{aligned} \kappa(x, y) &\geq \left(- \left(1 - \mu_x(y) - \mu_y(x) - \sum_{z, z \sim x, z \sim y} \mu_x(z) \vee \mu_y(z) \right)_+ \right. \\ &\quad \left. - \left(1 - \mu_x(y) - \mu_y(x) - \sum_{z, z \sim x, z \sim y} \mu_x(z) \wedge \mu_y(z) \right)_+ + \sum_{z, z \sim x, z \sim y} \mu_x(z) \wedge \mu_y(z) \right). \end{aligned}$$

□

Theorem 2. Let (X, d) be a space with metrics on \mathbb{Z} with a local probability measure $\mu_x(\cdot)$ for each $x \in X$. For any adjacent $x, y \in X$, let μ_x^α and μ_y^α be the lazy versions of μ_x and μ_y for the lazy parameter $\alpha \in (0, 1)$, respectively. Then,

$$W_1(\mu_x^\alpha, \mu_y^\alpha) \leq (1 - \alpha)W_1(\mu_x, \mu_y) + \alpha.$$

Proof. Let us denote γ as an optimal transport plan that realizes the infimum for $W_1(\mu_x, \mu_y)$. Let U be a random variable from the uniform distribution between $(0, 1)$. Let γ^α be a transport plan between μ_x^α and μ_y^α such that

$$\gamma^\alpha(x, y) = \begin{cases} (x, y) & \text{if } U < \alpha \\ \gamma(x, y) & \text{if } U \geq \alpha. \end{cases} \quad (7)$$

It is easy to see that γ^α is a valid transport plan between μ_x^α and μ_y^α since each marginal of γ^α is μ_x^α and μ_y^α , respectively. We can calculate the mass transferred under the plan γ^α by (5). With probability α , x and y keep their positions so the distance $d(x', y') = d(x, y) = 1$. On the other hand, with probability $1 - \alpha$, x and y moves according to the plan γ so the expected distance will be $W_1(\mu_x, \mu_y)$. Hence, the expected mass transferred under the plan γ^α is $\alpha + (1 - \alpha)W_1(\mu_x, \mu_y)$. For $W_1(\mu_x^\alpha, \mu_y^\alpha)$, we take the infimum over all possible transport plans, so $\alpha + (1 - \alpha)W_1(\mu_x, \mu_y)$ can be an upper bound of $W_1(\mu_x^\alpha, \mu_y^\alpha)$. \square

Corollary 1. *Let (X, d) be a space with metrics on \mathbb{Z} with a local probability measure $\mu_x(\cdot)$ for each $x \in X$. For any adjacent $x, y \in X$, let μ_x^α and μ_y^α be the lazy versions of μ_x and μ_y for the lazy parameter $\alpha \in (0, 1)$, respectively. Let $\kappa(x, y)$ be the Ricci curvature on (X, d, μ) and $\kappa^\alpha(x, y)$ be the Ricci curvature on (X, d, μ^α) between x and y , then*

$$\kappa^\alpha(x, y) \geq (1 - \alpha)\kappa(x, y). \quad (6)$$

Proof. From (2), we have

$$\kappa^\alpha(x, y) = 1 - W_1(\mu_x^\alpha, \mu_y^\alpha)$$

and Theorem 2 gives us an upper bound of $W_1(\mu_x^\alpha, \mu_y^\alpha)$ as

$$W_1(\mu_x^\alpha, \mu_y^\alpha) \leq (1 - \alpha)W_1(\mu_x, \mu_y) + \alpha.$$

Combining these two gives us

$$\begin{aligned} \kappa^\alpha(x, y) &= 1 - W_1(\mu_x^\alpha, \mu_y^\alpha) \geq 1 - ((1 - \alpha)W_1(\mu_x, \mu_y) + \alpha) \\ &= (1 - \alpha)(1 - W_1(\mu_x, \mu_y)) = (1 - \alpha)\kappa(x, y). \end{aligned}$$

\square

Theorem 3. *In a metric space (X, d) with metric $d(\cdot, \cdot)$ on \mathbb{Z} equipped with local probability measures $\mu_x(\cdot)$ for each point $x \in X$, for any adjacent pair of elements $x, y \in X$, without loss of generality assume $\mu_x(x) \leq \mu_y(y)$. $\mu_x(x)$ can be considered as laziness, and let ν_x and ν_y be the measures obtained by excluding laziness from μ_x and μ_y and renormalizing them. Then,*

$$\begin{aligned} W_1(\mu_x, \mu_y) &\leq \mu_x(x) + (1 - \mu_x(x)) \left(1 + \left(1 - \nu_x(y) - \nu_y(x) - \sum_{z, z \sim x, z \sim y} \nu_x(z) \vee \nu_y(z) \right)_+ \right. \\ &\quad \left. + \left(1 - \nu_x(y) - \nu_y(x) - \sum_{z, z \sim x, z \sim y} \nu_x(z) \wedge \nu_y(z) \right)_+ - \sum_{z, z \sim x, z \sim y} \nu_x(z) \wedge \nu_y(z) \right). \end{aligned}$$

Hence, we get

$$\begin{aligned} \kappa(x, y) &\geq (1 - \mu_x(x)) \left(- \left(1 - \nu_x(y) - \nu_y(x) - \sum_{z, z \sim x, z \sim y} \nu_x(z) \vee \nu_y(z) \right)_+ \right. \\ &\quad \left. - \left(1 - \nu_x(y) - \nu_y(x) - \sum_{z, z \sim x, z \sim y} \nu_x(z) \wedge \nu_y(z) \right)_+ + \sum_{z, z \sim x, z \sim y} \nu_x(z) \wedge \nu_y(z) \right). \end{aligned}$$

Proof. Define $\alpha = \mu_x(x)$. α can be considered as laziness for μ_x and μ_y , so we can obtain new probability measures ν_x and ν_y from μ_x and μ_y after removing the laziness and renormalizing. In other words,

$$\nu_x = \frac{1}{1 - \alpha} (\mu_x - \alpha\delta_x), \quad \nu_y = \frac{1}{1 - \alpha} (\mu_y - \alpha\delta_y).$$

We can interpret that μ_x and μ_y are lazy versions of ν_x and ν_y , respectively. Hence, we obtain

$$W_1(\mu_x, \mu_y) \leq (1 - \alpha)W_1(\nu_x, \nu_y) + \alpha \quad (8)$$

from Theorem 2. It remains to get $W_1(\nu_x, \nu_y)$. We obtain an upper bound of $W_1(\nu_x, \nu_y)$ by applying Theorem 1 to ν_x and ν_y .

$$W_1(\nu_x, \nu_y) \leq \left(1 + \left(1 - \nu_x(y) - \nu_y(x) - \sum_{z, z \sim x, z \sim y} \nu_x(z) \vee \nu_y(z) \right)_+ \right. \\ \left. + \left(1 - \nu_x(y) - \nu_y(x) - \sum_{z, z \sim x, z \sim y} \nu_x(z) \wedge \nu_y(z) \right)_+ - \sum_{z, z \sim x, z \sim y} \nu_x(z) \wedge \nu_y(z) \right).$$

By applying this upper bound to (8), we obtain the desired upper bound of $W_1(\mu_x, \mu_y)$. Combining this upper bound with (2), we obtain the desired lower bound of $\kappa(x, y)$. \square

A.2 Additional proofs

Theorem 4. *In a metric space (X, d) with metrics $d(\cdot, \cdot)$ on \mathbb{Z} equipped with local probability measures $\mu_x(\cdot)$ for each point $x \in X$, for any adjacent pair of elements $x, y \in X$,*

$$W_1(\mu_x, \mu_y) \leq 1 + 2(1 - \mu_x(y) - \mu_y(x))_+$$

Hence, we get

$$\kappa(x, y) \geq -2(1 - \mu_x(y) - \mu_y(x))_+$$

Proof. Using Kantorovich duality in Proposition 1, we get the following.

$$W_1(\mu_x, \mu_y) = \sup_{f, 1-Lip} \left(\sum_{z \sim x} f(z) \mu_x(z) - \sum_{z' \sim y} f(z') \mu_y(z') \right) \\ = \sup_{f, 1-Lip} \left(\sum_{z \sim x, z \neq y} (f(z) \mu_x(z) - f(x) \mu_x(x)) + (1 - \mu_x(y)) f(x) + f(y) \mu_x(y) \right. \\ \left. - \sum_{z' \sim y, z' \neq x} (f(z') \mu_y(z') - f(y) \mu_y(y)) - (1 - \mu_y(x)) f(y) - f(x) \mu_y(x) \right) \\ \leq (1 - \mu_x(y)) + (1 - \mu_y(x)) + |1 - \mu_x(y) - \mu_y(x)| \\ = 2 - \mu_x(y) - \mu_y(x) + |1 - \mu_x(y) - \mu_y(x)| \\ = 1 + 2(1 - \mu_x(y) - \mu_y(x))_+.$$

Therefore,

$$\kappa(x, y) \geq -2(1 - \mu_x(y) - \mu_y(x))_+.$$

\square

A.3 Wasserstein distance and Lower bounds on ORC on graphs

Theorem 5. *Let a locally finite graph be $G = (V, E)$. If x and y in V are neighboring vertices, we have the following.*

$$W_1(\mu_x, \mu_y) \leq 1 + \left(\left(1 - \mu_x(y) - \mu_y(x) - \sum_{z, z \sim x, z \sim y} \mu_x(z) \vee \mu_y(z) \right)_+ \right. \\ \left. + \left(1 - \mu_x(y) - \mu_y(x) - \sum_{z, z \sim x, z \sim y} \mu_x(z) \wedge \mu_y(z) \right)_+ - \sum_{z, z \sim x, z \sim y} \mu_x(z) \wedge \mu_y(z) \right).$$

Hence, we get

$$\begin{aligned} \kappa(x, y) \geq & \left(- \left(1 - \mu_x(y) - \mu_y(x) - \sum_{z, z \sim x, z \sim y} \mu_x(z) \vee \mu_y(z) \right) \right)_+ \\ & - \left(1 - \mu_x(y) - \mu_y(x) - \sum_{z, z \sim x, z \sim y} \mu_x(z) \wedge \mu_y(z) \right)_+ + \sum_{z, z \sim x, z \sim y} \mu_x(z) \wedge \mu_y(z) \end{aligned}$$

Proof. Apply Theorem 1 with the measure on locally finite graph. \square

So in weighted graph, we get the following result which is described in [10].

Theorem 6 (Theorem 6 in [10]). *Let $G = (V, E)$ be a locally finite graph. For any pair of adjacent vertices x, y ,*

$$\begin{aligned} W_1(\mu_x, \mu_y) \leq & 1 + \left(\left(1 - \frac{w_{xy}}{d_x} - \frac{w_{xy}}{d_y} - \sum_{x_1, x_1 \sim x, x_1 \sim y} \frac{w_{x_1x}}{d_x} \vee \frac{w_{x_1y}}{d_y} \right) \right)_+ \\ & + \left(1 - \frac{w_{xy}}{d_x} - \frac{w_{xy}}{d_y} - \sum_{x_1, x_1 \sim x, x_1 \sim y} \frac{w_{x_1x}}{d_x} \wedge \frac{w_{x_1y}}{d_y} \right)_+ - \sum_{x_1, x_1 \sim x, x_1 \sim y} \frac{w_{x_1x}}{d_x} \wedge \frac{w_{x_1y}}{d_y} \end{aligned}$$

Hence, we get

$$\begin{aligned} \kappa(x, y) \geq & \left(- \left(1 - \frac{w_{xy}}{d_x} - \frac{w_{xy}}{d_y} - \sum_{x_1, x_1 \sim x, x_1 \sim y} \frac{w_{x_1x}}{d_x} \vee \frac{w_{x_1y}}{d_y} \right) \right)_+ \\ & - \left(1 - \frac{w_{xy}}{d_x} - \frac{w_{xy}}{d_y} - \sum_{x_1, x_1 \sim x, x_1 \sim y} \frac{w_{x_1x}}{d_x} \wedge \frac{w_{x_1y}}{d_y} \right)_+ + \sum_{x_1, x_1 \sim x, x_1 \sim y} \frac{w_{x_1x}}{d_x} \wedge \frac{w_{x_1y}}{d_y} \end{aligned}$$

For α -lazy version, we can derive the following.

Theorem 7. *Let $G = (V, E)$ be a locally finite graph. For any pair of adjacent vertices x, y ,*

$$\begin{aligned} \kappa(x, y) \geq & (1 - \alpha) \left(- \left(1 - \frac{w_{xy}}{d_x} - \frac{w_{xy}}{d_y} - \sum_{x_1, x_1 \sim x, x_1 \sim y} \frac{w_{x_1x}}{d_x} \vee \frac{w_{x_1y}}{d_y} \right) \right)_+ \\ & - \left(1 - \frac{w_{xy}}{d_x} - \frac{w_{xy}}{d_y} - \sum_{x_1, x_1 \sim x, x_1 \sim y} \frac{w_{x_1x}}{d_x} \wedge \frac{w_{x_1y}}{d_y} \right)_+ + \sum_{x_1, x_1 \sim x, x_1 \sim y} \frac{w_{x_1x}}{d_x} \wedge \frac{w_{x_1y}}{d_y} \end{aligned}$$

B Curvatures in Hypergraphs

As mentioned in Section 5, Coupette et al. [5] proposed a framework for describing curvature in hypergraphs. This framework is divided into three main parts: first, defining the local measures from a given hypergraph; second, introducing the aggregate function, a new function that plays the role of the Wasserstein distance in hypergraphs; and third, defining multiple curvatures, not just for a single edge.

First, let us discuss the local measures. There are various ways to define the local measures. The following three methods are representative examples. First, the Equal-Nodes Random Walk approach assigns equal probability mass to the neighborhood $\mathcal{N}(x)$ of a vertex x , regardless of the complexity of the edges containing x . Thus, for x and y with $x \sim y$, the probability of moving from x to y is

$$\mu_x^{EN}(y) = \frac{1}{|\mathcal{N}(x)|}.$$

Second, the Equal-Edges Random Walk method involves uniformly selecting an edge e that includes a given vertex x and then uniformly selecting a vertex y in that chosen edge e . For adjacent x and y , we can define the probability of moving x to y as

$$\mu_x^{EE}(y) = \frac{1}{\deg(x) - |\{e \ni x \mid |e| = 1\}|} \sum_{e \ni \{x,y\}} \frac{1}{|e| - 1}.$$

Third, the Weighted-Edges Random Walk approach selects an edge e in proportion to its cardinality before selecting a new vertex u . After picking e , it chooses a vertex u . For adjacent x and y , the probability of moving x to y is

$$\mu_x^{WE}(y) = \sum_{e \ni \{x,y\}} \frac{|e| - 1}{\sum_{f \ni x} (|f| - 1)} \frac{1}{|e| - 1}.$$

Next, we introduce the three aggregate functions mentioned earlier. First, the AGG_A function calculates the average of the Wasserstein distances for all pairs of vertices within an edge.

$$AGG_A(e) = \frac{2}{|e|(|e| - 1)} \sum_{\{i,j\} \subseteq e} W_1(\mu_i, \mu_j)$$

The AGG_B function calculates the average Wasserstein distance between the local measures of all vertices within an edge and the barycentric measure of these local measures.

$$AGG_B(e) = \frac{1}{|e| - 1} \sum_{i \in e} W_1(\mu_i, \bar{\mu})$$

where $\bar{\mu}$ denotes the barycenter of the probability measures of nodes contained in e , i.e., the distribution $\bar{\mu}$ that minimizes the value of $\sum_{i \in e} W_1(\mu_i, \bar{\mu})$.

Finally, the AGG_M function returns the maximum Wasserstein distance among all pairs of vertices within a given edge.

$$AGG_M(e) = \max\{W_1(\mu_i, \mu_j) \mid \{i, j\} \subseteq e\}$$

The AGG_M function, which simply returns the maximum Wasserstein distance among all pairs of vertices within an edge, is less effective compared to the average (AGG_A) or barycenter (AGG_B) methods. The AGG_M function does not provide as comprehensive a measure of the distribution of distances as the other methods.

Moreover, while AGG_B has a clear mathematical interpretation through the barycentric measure, it incurs additional computational costs due to the need to determine the barycentric measure. Consequently, AGG_A , which calculates the average Wasserstein distance, is preferred for simulations due to its balance between computational efficiency and informative value.

Curvature can be discussed not only for edges but also for nodes [2; 10]. In hypergraphs, there are several ways to define curvatures for a vertex i . One is as the mean of all curvatures between a vertex i and the neighborhood $\mathcal{N}(i)$ of i . We will note it as node curvature at i with the neighborhood:

$$\kappa^{\mathcal{N}}(i) = \frac{1}{|\mathcal{N}(i)|} \sum_{j \in \mathcal{N}(i)} \kappa(i, j)$$

Secondly, it can be derived as the mean of all curvatures of edges containing a vertex i . In short, we will note this as node curvature at i with edges:

$$\kappa^E(i) = \frac{1}{\deg(i)} \sum_{e \ni i} \kappa(e)$$

C Experiment Details

C.1 Datasets

For our experiments, we utilized a subset of the datasets released by Coupette et al. in their paper [5]. These datasets are publicly available², and we have directly used some of them in our study. Below is a brief description of each dataset we employed.

C.1.1 NDC-AI, NDC-PC: Drugs Approved by the U.S. Food and Drug Administration

The U.S. Food and Drug Administration (FDA) gathers data on all pharmaceuticals produced, prepared, propagated, compounded, or processed by registered drug establishments for commercial distribution within the United States. This information is maintained in the National Drug Code (NDC) Directory, which is updated daily and contains listed NDC numbers and all related drug information. From this CSV file, they derived two hypergraphs: *ndc-ai*, where nodes represent active ingredients used in these drugs, and *ndc-pc*, where nodes correspond to the pharmaceutical classes assigned to these drugs. In both hypergraphs, edges represent FDA-registered drugs.

C.1.2 MUS: Music Pieces

The music21 library is an open-source Python tool for computer-aided musicology that includes a corpus of public-domain music in symbolic notation. They used music21 to extract hypergraphs from this corpus. Each hypergraph represents a music piece, with edges corresponding to chords played for specific durations and nodes representing sound frequencies. Unlike other collections, the hypergraphs in the mus collection are node-aligned. Edges with cardinality 0, corresponding to pauses, were included in the cardinality decomposition but excluded from curvature computations. This dataset contains 1944 hypergraphs.

C.1.3 STEX: StackExchange Sites

StackExchange hosts Q&A communities, where each question is tagged with at least one and at most five tags. The data covers associated tags and other metadata (including question titles and, for smaller sites, the question bodies). From this data, they created the stex hypergraph collection, where each hypergraph represents a StackExchange site, each edge represents a question, and each node represents a tag used at least once on that site. This dataset contains 355 hypergraphs.

C.1.4 SHA: Shakespeare's Plays

The sha collection is a subset of the HYPERBARD dataset recently introduced by Coupette et al.[6], based on the TEI-encoded XML files of Shakespeare's plays provided by Folger Digital Texts. In this dataset, each hypergraph represents one of Shakespeare's plays, categorized into three types: comedy, history, and tragedy. In each hypergraph, nodes correspond to named characters in the play, and edges represent groups of characters who are simultaneously present on stage. This dataset contains 37 hypergraphs.

C.1.5 SYN_HCM, SYN_HSBM, SYN_HCM-HSBM: Synthetic Hypergraphs

To generate synthetic hypergraphs, they developed hypergraph generators that extend three well-known graph models to hypergraphs. For the *syn_hcm* data, they adapted the configuration model, which, in the context of undirected graphs, is defined by a degree sequence. Our hypergraph configuration model is characterized by both a node degree sequence and an edge cardinality sequence. Similarly, for the *syn_hsbm* data, they extended the stochastic block model, which, for undirected graphs, is defined by a vector of c community sizes and a $c \times c$ affinity matrix that specifies affiliation probabilities between communities. Our hypergraph stochastic block model is defined by a vector of c_V node community sizes, a vector of c_E edge community sizes, and a $c_V \times c_E$ affinity matrix that specifies the affiliation probabilities between node communities and edge communities.

They used each of our generators to create 250 hypergraphs for *syn_hcm* and *syn_hsbm* with identical node count n , edge count m , and density $c = nm$, where c is the number of filled cells in the

²<https://doi.org/10.5281/zenodo.7624573>

node-to-edge incidence matrix. Also, they generated a mixture of data, noted `syn_hcm-hsbm`, with 500 hypergraphs based on each dataset.

C.2 Experimental Setup

First, we will explain the experimental setting. Regarding the time evaluation discussed in Section (6.1), we performed the following steps for each dataset:

1. Constructed the local measure using the Weighted-Edges Random Walk method and estimated the AGG_A function.
2. Constructed the local measure using the Equal-Nodes Random Walk method and estimated the AGG_A function.

The time taken for these steps was measured, focusing specifically on the time required for computing the Wasserstein distance, as this is the primary difference between the traditional and our methods.

Regarding the curvature evaluations discussed in Section 2, for each dataset, we constructed the local measure using the Equal-Nodes Random Walk method and estimated the AGG_A function. We then measured the edge curvature and the two types of node curvatures introduced in Appendix B.

Given our development focuses on the calculation of the Wasserstein distance, we only modified the function of calculating Wasserstein distance in the publicly available code³ by Coupette et al. [5] according to our algorithm in Algorithm 1. In their code, the Sinkhorn algorithm provided by an open library was used to compute the Wasserstein distance. Parameters such as the number of iterations and a convergence radius set to 500 and 1/100, respectively. Based on the algorithm we proposed in Algorithm 1, we calculated the Wasserstein distance, then measured the computation time and compared the resulting curvatures.

Our experiments were performed on a computer with Intel(R) Core(TM) i5-9600 CPU @ 3.10GHz and 16.0GB RAM. Initially, we intended to run experiments on all datasets publicly available from Coupette et al. [5]. However, some large-scale datasets caused our computing worker to run out of RAM, resulting in segmentation fault errors, or the traditional numerical algorithm failing to converge. Therefore, we had to limit our experiments to datasets that were feasible to test within our environment. Although we could not perform tests on the entire dataset, our claims were validated on the remaining feasible data, and we considered this to be sufficient.

³<https://doi.org/10.5281/zenodo.7624573>